Roman HAMAR, Pavel TRNKA

University of West Bohemia

Gliding discharges in rotary machine insulation – diagnostics, simulation and measurement

Abstract. *The issue of discharge activity is constantly encountered when operating electric devices of higher performances as well as higher working voltages. This paper provides a study of conditions in the stressed place of an insulation system, i.e. in a conductor outlet from a rotary machine stator slot. The simulation of an electric field distribution presented in this article is aimed to match reality as closely as possible. The trouble spot is located by both an electric field simulation and a practical measurement.*

Streszczenie. *Wyładowania pełzające pojawiają się w urządzeniach elektrycznych o wysokiej sprawności oraz w urządzeniach wysokonapięciowych. W tej pracy omówiono warunki w narażonym systemie izolacji to jest w wyprowadzeniu przewodu ze żłobka statora maszyny wirującej. Przez możliwie realistyczną symulacja pola elektrycznego udało się zlokalizować miejsce narażenia potwierdzone praktycznymi pomiarami. (**Wyładowania pełzające w izolacji maszyn elektrycznych**)*

Keywords: gliding discharges, insulation degradation, computer simulation, rotary machines.
Słowa kluczowe: wyładowania pełzające, izolacja, maszyny wirujące

Introduction

Electric rotary machines of high power and high voltage, such as turbo generators and hydro generators, are typical of gliding discharge occurrence in places where insulated stator bars stick out from slots [1, 2]. This issue has not been investigated sufficiently as far as rotary machines of lower outputs are concerned.

Consider a drive with a frequency converter, where the asynchronous motor is directly controlled and supplied from this converter. In such a drive, the stator insulation system is stressed with rather steep voltage impulses. If we consider a mains supply of 3x400 V, then the capacitor in the DC part of the inverter circuit is charged to approximately 560 V. The fast switching components of the inverter modulate this voltage and the voltage impulses on the inverter output are virtually of this voltage value. There occur reflections in the cable located between the load, i.e. the motor, and the inverter output terminals. Because of the steep voltage impulses, which correspond to frequencies of MHz order, it is necessary to consider this cable as a distributed parameter line. Due to the reflections, the voltage on the load can sometimes reach values two times to manifold higher than the voltage in the DC part of the inverter circuit. This value exceeds the value of inception voltage U_i (kV) even at the feed of 3x400 V. Corona inception voltage of such an insulation is somewhere over 1 kV. As motors of medium performance (e.g. a tram) are fed with a higher voltage, the occurrence of discharge activity in these motors is highly probable.

Experiment

Picture 1 shows a sample of a motor winding which consists of an internal copper electrode, electrical insulation 1 mm thick and an external aluminium electrode. The internal electrode represents the winding conductor and the external electrode represents the magnetic circuit of the machine.

The sample has been designed so that its shape corresponded to a real motor winding. Similarly to practice, the insulation system has been created by using the vacuum pressure impregnation technology (VPI technology). There has been applied a three-component composite material which is normally used for manufacturing the main insulations of rotary machines. The parameters of the electrical insulation are as follows: relative permittivity ε_r = 2.8 and specific resistance ρ = $2 \cdot 10^{14}$ Ωm.

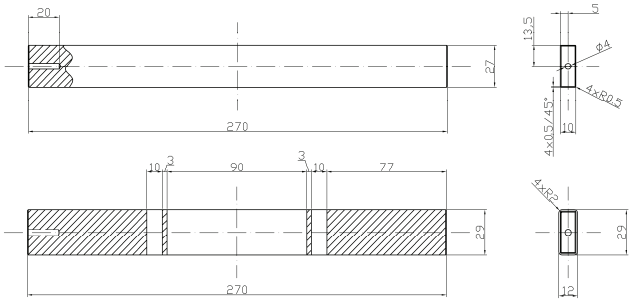

Fig.1. Motor Winding Sample

In order to simulate the influence of operational voltage, the samples were stressed with a pulse voltage which was supplied to the internal electrode (i.e. the copper bar). The external electrode (the aluminium foil) was grounded. This was applied for both the computer model of the electric field and the practical experiment verifying the sample aging by using the pulse voltage in a laboratory. Fig. 2 depicts the course of the pulse voltage. The picture on the left shows the pulse course recorded by an oscilloscope and the picture on the right depicts approximation of this course. The parameters of the pulse voltage were ± 1.5 kV, 6 kHz, 50 % duty cycle. The approximated shape of the pulse was then used to calculate numerically the non-stationary electric field in this insulation.

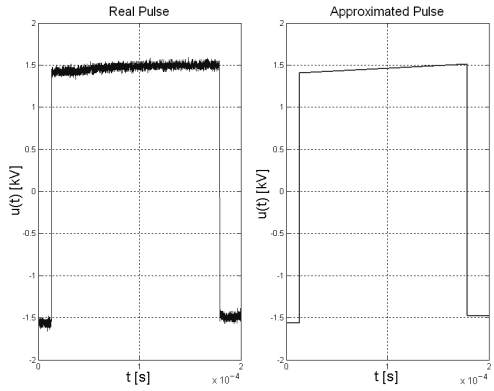

Fig.2. Voltage pulse

In its centre of gravity, the motor winding sample is axisymmetric according to the *x*, *y* and *z* axes, so it was enough to simulate just its symmetric eighth. However, computation of the non-stationary electric field for the entire

eighth of the sample would have been numerically demanding and even useless from the point of view of electric field gradient [3, 4]. For this reason, an undemanding calculation of an electrostatic field of the entire eighth was first performed. Consequently, there was performed an analysis whose purpose was to find out which part of the sample's eighth would be sufficient for the calculation of the non-stationary electric field. The results of this analysis showed that in order to calculate the non-stationary electric field of the given sample, it would be enough to simulate a small area at the boundary between the external electrode and the insulation. Fig. 3 shows the simulated part viewed from the outer part of the insulation, where the external electrode is depicted dark. The internal electrode is not viewed from this angle. This small part of the specimen is demarcated by the 4 mm length of the insulation with the external electrode + the 4 mm length of the insulation without the external electrode. Therefore, the length of the insulation in the demarcated area is 8 mm in total.

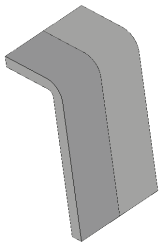

Fig.3. Simulated part of the insulation viewed from the outside

The propagation of non-stationary electromagnetic field in this insulation of the permittivity ε, permeability μ and the conductivity γ is described by means of differential equation for the electric potential φ:

$$\nabla^2\varphi - \mu\,\varepsilon\,\frac{\partial^2\varphi}{\partial t^2} - \mu\,\gamma\,\frac{\partial\varphi}{\partial t} = 0 \tag{1}$$

The initial conditions for the entire insulation area were zero. The boundary condition for the external electrode was φ = 0 V. The boundary condition for the internal electrode was a given continuous function of time (see Fig. 2). This time function was put into the COMSOL program by means of table.

The numerical computation was performed using the 3.4 version of the COMSOL program launched by the COMSOL AB corporation (www.comsol.com) by means of the finite element method. The created model contained approximately 150 thousand elements. Depending on the time course of the pulse, there were created animations representing the distribution of electric potential and electric field strength in the insulation.

Pictures 4 to 8 were created for time $1.7\cdot10^{-4}$ s when the calculated electric field strength in the insulation reached the peak values. Fig. 4 shows the electric field potential distribution for the specimen viewed from the outside. As the colour scale indicates, in the given time the electric potential of the internal electrode is 1508 volts and the external electrode is grounded. Fig. 5 depicts electric potential in individual slices of the insulation. The distance between individual slices was set at 1.5 mm. Fig. 6 shows electric field strength distribution in the insulation being viewed from the outside. The picture indicates that the peak value of the electric field intensity, 4.75 kV/mm, is located on the boundary between the external electrode and the insulation. Such a high value of the electric field strength is only found on the outer surface of the insulation, which is supported by Fig. 7, where the sample's insulation is viewed from the inside. The picture also shows the insulation cross-section in xy plane. It also follows from fig. 7 that in the bend of the insulation adjacent to the internal electrode, or rather in the section located under the external electrode, the value of the electric field intensity is increased to 2.5 kV/mm. The individual slices in Fig. 8 clearly show that the highest value of the electric field strength, namely 4.75 kV/mm, is located on the boundary between the external electrode and the insulation.

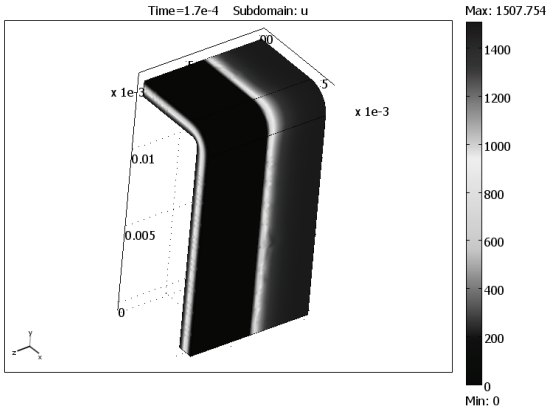

Fig.4. Electric potential viewed from the outside

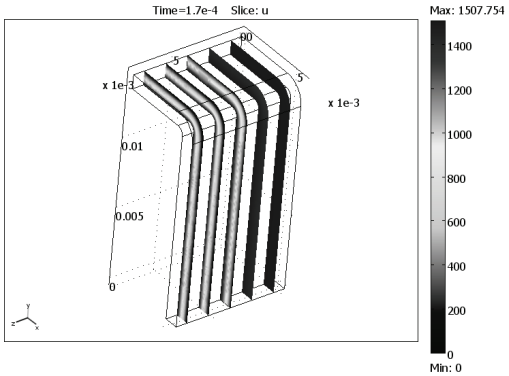

Fig.5. Electric potential in individual slices of the insulation

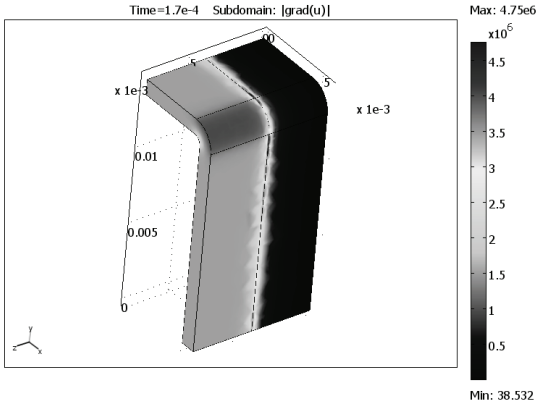

Fig.6. Electric field strength viewed from the outside

As the performed simulation (see Fig. 6 and 8) suggests, the highest electric field strength is located in place where the winding outlet from the stator slot has been simulated. The computed value of the electric field strength in this place indicates the probability of gliding discharges occurrence, which may result in escalated degradation of electrical insulation in this problematic place.

Subjecting the sample to a pulse voltage for 500 hours resulted in degradation of the electrical insulation in this place. The degradation is clearly shown in Fig. 9ab. Picture

a) depicts a detail of the problematic place before the exposition and picture b) shows the same area after the exposition.

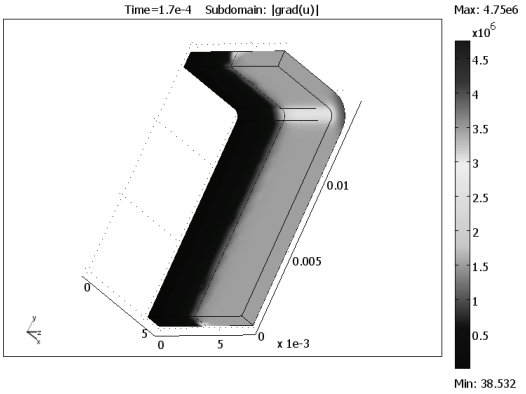

Fig.7. Electric field strength viewed from the inside

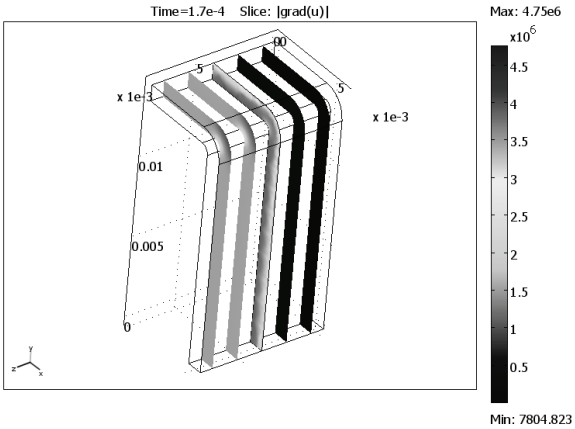

Fig.8. Electric field strength in individual slices of the insulation

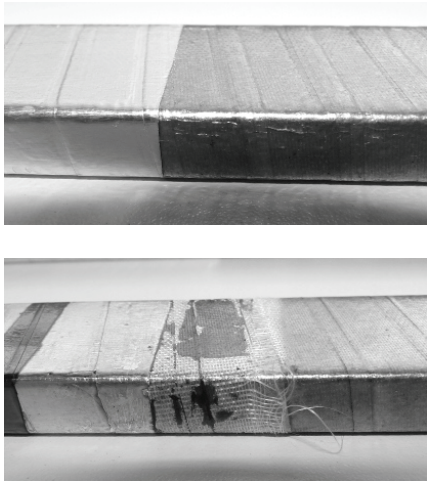

a)

b)

Fig.9. The sample of electric motor insulation system a) before the exposition, b) after the exposition – visible degradation of the three-component composite bond, bare bearing component

Partial discharges measurement

Partial discharges measurement of samples can help easily detect the gliding discharges occurrence in the given arrangement. This is clearly seen in Fig. 10. The PD pattern suggests partial discharge activity approximately between 60° and 180° on the voltage phase used for the measurement. This indicates the occurrence of the gliding discharges anticipated by the calculation.

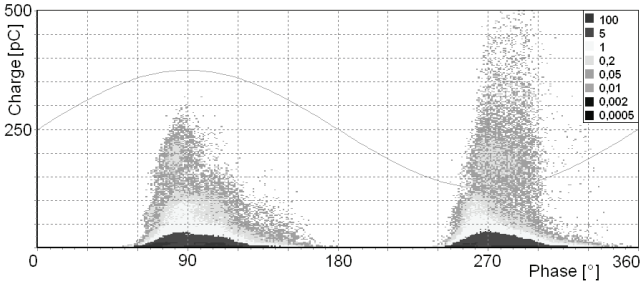

Fig.10. PD Pattern of measured sample

Conclusion

It has always been necessary and needed to identify precisely the most stressed spots in an insulation system. As this article has suggested, the anticipated problematic place in an insulation system can be easily identified by using a computer simulation. This has been verified by a practical measurement. A sample, whose dimensions and stressing corresponded to the computer simulation, was after exposition clearly degraded in exactly the place the simulation had indicated. A high value of the electric field strength on the boundary between the external electrode and the insulation is a source of gliding discharges depending on the value of the internal electrode voltage. Thus degradation activity is initiated, which can lead to the electrical insulation breakdown. As the presented experiment shows, such degradation may occur even in an insulation system of a motor fed from a lower voltage source. Another dangerous spot as far as insulation degradation is concerned, is the bend of the insulation adjacent to the internal electrode (winding conductor of a rotary machine), or rather in the part located under the external electrode. This place is not located on the surface; therefore, a computer simulation is the only nondestructive diagnostic means applicable for such an inaccessible place.

Acknowledgment

Financial support of the Research Plan MSM 4977751310 is gratefully acknowledged.

REFERENCES

[1] Espino-Cortes F.P., Jayaram S.H., Cherney E.A., Effectiveness of Stress Control Coatings in Medium Voltage Form Wound Coils Ends under Fast Rise Time Pulses and Contamination, *Electrical Insulation Conference and Electrical Manufacturing Expo*, 2005, 167-170

[2] Mentlík V., Trnka P., Pihera J., Hamar R., Zvýšení provozní spolehlivosti motorů s měniči s rychlými spínacími prvky, *Elektro*, 18 (2008), ISSN 1210-0889, No. 12, 4-8

[3] Hamar R., Mentlík V., Ulrych, B., Transient phenomena in the imperfect dielectric. *AMTEE'05*, 2005, ISBN 80-7043-392-2, 27-34

[4] Hamar R., The Application of the MATLAB and COMSOL Programs for the Computation of a 3D Non-stationary Electric Field, *AMTEE'09*, 2009, ISBN 978-80-7043-821-3, 1-4

***Authors**: Ing. Roman Hamar, Ph.D.; Doc. Ing. Pavel Trnka, Ph.D., University of West Bohemia, Faculty of Electrical Engineering, Univerzitní 26, 30614 Plzeň, E-mail: hamar@kte.zcu.cz; pavel@ket.zcu.cz.*